Tumor cell-derived CCL2 promotes chemoresistance via c-Fos in lung adenocarcinoma

Dong Wang
Zhengzhou University First Affiliated Hospital
Li Yang
Zhengzhou University First Affiliated Hospital
Yanjun Li
Zhengzhou University First Affiliated Hospital
Ling Cao
Zhengzhou University First Affiliated Hospital
Kai Zhang
Zhengzhou University First Affiliated Hospital
Jingyao Lian
Zhengzhou University First Affiliated Hospital
Zhibo Shen
Zhengzhou University First Affiliated Hospital
Jianmin Huang
Zhengzhou University First Affiliated Hospital
Liping Wang
Zhengzhou University First Affiliated Hospital
Yi Zhang (yizhang@zzu.edu.cn)
Zhengzhou University First Affiliated Hospital https://orcid.org/0000-0001-9861-4681

Primary research

Keywords: Chemoresistance, CCL2, c-Fos, Macrophage, Lung adenocarcinoma

Posted Date: May 5th, 2021

DOI: https://doi.org/10.21203/rs.3.rs-450308/v1

Abstract

Background

The tumor microenvironment plays an important role in promoting chemoresistance in solid cancers. This study aimed to evaluate the underlying molecular mechanisms in the tumor microenvironment potentially involved in chemoresistance in lung adenocarcinoma patients.

Methods

A multiplex assay was used to determine the transcription factor levels in chemoresistant lung adenocarcinoma cells. The role of chemokine (C-C motif) ligand 2 (CCL2) in chemoresistance of lung adenocarcinoma was evaluated both *in vitro* and *in vivo*. A ChIP assay was performed to determine the molecular mechanism by which c-Fos regulates “CCL2”.

Results

CCL2 expression was significantly higher in chemoresistant than in chemosensitive lung adenocarcinoma cells and was closely associated with poor survival in lung adenocarcinoma patients. CCL2 enhanced the resistance of lung adenocarcinoma cells to cisplatin *in vitro*. Chemoresistant lung adenocarcinoma cell-derived CCL2 promoted monocyte recruitment to the tumor site and monocyte polarization into M2 macrophages, which further mediated the chemoresistance of lung adenocarcinoma. The involvement of c-Fos in CCL2 expression in lung adenocarcinoma cells might promote chemoresistance. Blockade of CCL2 suppressed tumor growth and restored cisplatin sensitivity in lung adenocarcinoma.

Conclusions

The c-Fos–CCL2 axis might provide a promising target for the treatment of lung adenocarcinoma.

Introduction

One of the main causes of treatment failure in cancer patients is resistance to chemotherapy [1, 2]. Although there are many studies on the mechanisms underlying anticancer drug resistance, these mechanisms are not fully understood. In recent years, there has been increasing evidence that the tumor microenvironment (TME) plays a key role in the occurrence of chemotherapy resistance in solid tumors [3, 4].

Various factors can lead to resistance in the immunosuppressive TME. In metastatic renal cell carcinoma, the higher infiltration of $CD4^{+}FOXP3^{+}$ regulatory T cells may be closely related to resistance to

antiangiogenic therapy [5]. Tumor-associated macrophage-derived inducible nitric oxide synthase protected tumor cells from chemotherapeutic drug-induced apoptosis [6]. In addition, chemokines, including CXCL12 (C-X-C motif chemokine 12), play an important role in supporting cancer cell survival and promoting drug resistance [7–9]. Anti-apoptotic molecules, including IL-6, IL-10, and TNF-α, were involved in promoting the chemoresistance of non-Hodgkin's lymphoma, breast cancer, and glioma [10–13]. We previously reported the importance of CXCR7 in controlling IL-6-induced cancer-cell proliferation and chemoresistance in esophageal squamous cell carcinoma. Therefore, the underlying molecular mechanisms whereby the TME regulates drug resistance provide potential targets to overcome resistance.

Lung adenocarcinoma is the most common type of lung cancer in non-small-cell lung cancer. Current research suggests that genetic factors, second-hand smoke, and exposure to sputum in the home play key roles in the development of lung cancer, but the specific reasons remain unclear. Most commonly, treatment for patients with advanced lung adenocarcinoma begins with either cisplatin or carboplatin combined with another medication. It is necessary to reverse drug resistance in order to improve the clinical prognosis of these patients.

Here, we found that the expression levels of chemokine (C-C motif) ligand 2 (CCL2) in cisplatin-resistant A549/Cis cells and tumor tissues of patients with cisplatin resistance were significantly higher than in controls. CCL2 expression was closely associated with poor prognosis in lung adenocarcinoma patients, and may therefore serve as a potential biomarker for the prognosis of lung adenocarcinoma. CCL2 enhanced cisplatin-resistance in A549 cells via c-Fos. Moreover, A549/Cis cell-derived CCL2 promoted the recruitment and polarization of monocytes into M2 macrophages, which further induced chemoresistance. This study demonstrates the importance of CCL2 in controlling chemoresistance induced by c-Fos in lung adenocarcinoma. The c-Fos-CCL2 axis is a potential molecular target for lung adenocarcinoma therapy.

Materials And Methods

Patients and tumor samples

Eighty-one lung adenocarcinoma tissue samples were obtained from The First Affiliated Hospital of Zhengzhou University and were used for immunohistochemical analysis. All patient diagnoses were confirmed by pathological analysis and then staged according to the TNM system. The study was approved by the Ethics Committee of our hospital, and all patients signed a written informed-consent form.

Multiplex assay

To identify which factors play key roles in determining and maintaining chemoresistance in lung adenocarcinoma cells, a multiplex assay was used. Cytokine and chemokine levels (for 13 human

cytokines and 13 human chemokines) in the supernatants of A549 and A549/Cis cells were analyzed using a Multianalyte Flow Assay Kit (BioLegend, USA), according to the manufacturer's instructions.

RNA extraction and qPCR

Total RNA was extracted from cells and tissues. RNA concentration and purity were then measured using a NanoDrop 2000 (Thermo Scientific, USA). Total RNA was reverse transcribed into cDNA using a reverse transcription kit (TaKaRa, Japan). qPCR was performed using SYBR Premix Ex Taq II (TaKaRa, Japan) in the Agilent Mx3005P system. GAPDH was used as an endogenous control for normalization.

ELISA

The concentration of CCL2 in the supernatants of A549 and A549/Cis cells, and in the supernatants of tissue samples from lung adenocarcinoma patients, was measured by ELISA (R&D Systems Inc., USA), as previously described [14].

Immunohistochemistry

The expression of CCL2 in paraffin-embedded tissue samples from 81 lung adenocarcinoma patients was examined. The primary antibody (anti-CCL2, 1:200; Abcam, USA) was incubated overnight at 4 °C. The secondary antibody was incubated at 37 °C for 1 h. The incubated samples were then counterstained with hematoxylin and observed under a microscope (Olympus, Japan). Each sample was selected using three fields of view.

Lentiviral generation and cell sorting

The gene sequence of interest was stably transfected into A549/Cis cells using a lentiviral vector, and the expression of CCL2 was confirmed by qPCR and western blotting. All inserted sequences were confirmed by DNA sequencing. After 48 h, cells expressing green fluorescent protein (GFP) were sorted by flow cytometry (MoFlo XDP, Beckman Coulter, USA).

Cell lines and cell culture conditions

Human non-small cell lung cancer cell line A549, cisplatin resistant cell line A549/Cis and HUVEC were purchased from the Institute of basic medicine, Chinese Academy of Medical Sciences. The cells were cultured in DMEM high glucose medium containing 10% fetal bovine serum (FBS, Hyclone) at 37 ℃ and 5% CO2. The growth was observed regularly, and the medium was changed and digested for passage. All cells were tested in logarithmic growth phase.

Cell viability assay

Cell proliferation rate was determined by CCK8 assay (Dojindo, Japan) according to the manufacturer's protocol. Cells were seeded in five replicates in a 96-well plate at a density of 5,000 cells per well. The cells were cultured with 100 μL Dulbecco's Modified Eagle Medium (DMEM) containing 10 % FBS. Cells

were incubated with 10 μL of CCK-8 for 4 h at 37 °C. Viable cells were counted every day by reading the absorbance at 450 nm with a plate reader (Multiskan MK3, Thermo Scientific, USA).

Flow cytometrical evaluation of apoptosis

After treatment with cisplatin (also known as DDP), A549/Cis and shCCL2 cells were harvested. Cell concentration was then adjusted to 10^6 cells/mL. Cells were incubated with Alexa Fluor 647 Annexin V (BioLegend, USA) for 15 min in the dark, and samples were analyzed by flow cytometry (FACSCanto II, BD Biosciences, USA) immediately after addition of PI (Sigma, USA).

Sphere-formation assay

A549/Cis or shCCL2 cells (5×10^3 cells/well) were seeded in ultra-low-attachment 24-well plates (Corning, USA) for pellet-formation assay, and were cultured in pellet culture medium (containing B27 supplement (Gibco, USA), EGF (20 ng/mL; Peprotech, USA), and bFGF (20 ng/mL; Peprotech, USA), in DMEM and F12 media (Sigma, USA). After 7 d, spheres with a diameter > 75 μm were counted.

Migration assay

A 0.4 μm diameter chamber (Corning, USA) was used in a transwell assay, whereby 1×10^5 THP-1 cells were seeded in the upper chamber, and 600 μL of A549 or A549/Cis cell supernatants were co-cultured in the bottom chamber. CCL2 inhibitor (Selleck, China) was included in these cells. The cells were incubated at 5 % CO_2 and 37 °C for 48 h. The change in the percentage of $CD14^+CD163^+$ cells, and the expression of inflammatory cytokine genes, was measured.

In another migration assay, 5×10^4 A549 or A549/Cis cells were seeded in the upper chamber with 600 μL of M2 macrophage supernatant using an 8 μm diameter chamber (Corning, USA). After 24 h incubation, the migrated cells stained with 0.1 % crystal violet were counted. All experiments were repeated independently three times.

Tube-formation assay

Subconfluent human umbilical vein endothelial cells (HUVECs) were harvested resuspended in the A549 or A549/Cis co-cultured with M2 macrophages supernatants. This suspension was seeded (3×10^4 cells/well) in BD Matrigel (Becton Dickinson, USA) in a 96-well plate, and incubated for 3 h at 5 % CO_2 and 37 °C. Tube formation was examined under an inverted microscope.

RT^2 profiler PCR array

Total RNA was isolated from A549 and A549/Cis cells according to the manufacturer's instructions (QIAGEN, Germany). Detailed RT^2 profiler PCR array experiments were performed as previously described [15].

ChIP and qChIP assay

A ChIP assay was performed with 2.5 μg anti-CCL2 and goat anti-rabbit IgG (Cell Signaling Technology, USA) as the negative controls, using a Simple ChIP Enzymatic Chromatin IP Kit (Cell Signaling Technology, USA) according to the manufacturer's protocol. The following *c-Fos* primers were used: forward, 5'- AACCTAACGAAAGCTGGGTTG-3'; reverse, 5'- AATGGCATTGTTGAGTGCAT-3'. Detailed ChIP and qChIP assay experiments were performed as previously described [15].

Animal model

Twenty-four 6-week-old female NOD SCID mice (Beijing Vital River Experimental Animal Science and Technology Co., Ltd.) were randomly divided into six groups (four mice/group). The two groups were injected subcutaneously with shRNA control or shCCL2 A549/Cis cells (5×10^6 cells resuspended in 100 μL PBS). Tumor growth was assessed by measuring the length and width of the tumor mass with a Vernier caliper. When the tumor volume reached 250 mm^3, treatment with cisplatin (3 mg/kg once a week, i.p.) was started. Human $CD14^+$ cells (5×10^6 cells) were transplanted through the tail vein 3 d before the mice were sacrificed. Three days after transplantation of human CD14 + cells into tail vein, mice were sacrificed by intraperitoneal injection of pentobarbital sodium 150mg / kg. All animal experiments were approved by the Institutional Animal Care and Use Committee of the First Affiliated Hospital of Zhengzhou University.

Statistical analysis

Data were analyzed using Student's *t*-tests or chi-square tests, and are reported as means ± SD. The overall survival curve was plotted using the Kaplan-Meier method. Statistical analysis was performed using GraphPad Prism 7 (La Jolla, CA, USA). Differences were considered statistically significant at $P < 0.05$.

Results

CCL2 level is elevated in chemoresistant lung adenocarcinoma cells

To confirm that A549/Cis cells are the chemoresistant lung adenocarcinoma cells, we first compared the expression of chemoresistance-related genes in A549 (cisplatin-sensitive) and A549/Cis (cisplatin-resistant) cells by qPCR. Expression of these genes was higher in A549/Cis cells than in A549 cells ($P < 0.05$, Figure 1A). To determine the dominant factor involved in chemoresistance, the expression levels of several chemokines and cytokines in the supernatants of A549 and A549/Cis cells were detected by multiplex assay. We found that the CCL2 level was significantly higher in the supernatants of A549/Cis cells than in those of A549 cells (Figure 1B). The other cytokines and chemokines did not show significant differences. To confirm this result, we further detected the mRNA and protein expression of CCL2 in the A549 and A549/Cis cells by qPCR, and in their supernatants by ELISA. Similarly, CCL2 mRNA expression was markedly higher in A549/Cis cells than in A549 cells ($P < 0.01$, Figure 1C), and the CCL2

protein level in the A549/Cis cell supernatants was significantly higher than in the A549 cell supernatants ($P < 0.001$, Figure 1D). Therefore, these results suggest that the level of CCL2 is elevated in chemoresistant lung adenocarcinoma cells.

High CCL2 levels are closely associated with chemoresistance and poor survival in lung adenocarcinoma patients

To further investigate the association between CCL2 and chemoresistance in lung adenocarcinoma patients, CCL2 expression in chemosensitive and chemoresistant patients was assessed by immunohistochemical analysis. The level of CCL2 was significantly higher in chemoresistant patients than in chemosensitive patients ($P < 0.01$, Figure 2A). The association between CCL2 expression and clinicopathologic characteristics is shown in Table 1. In addition, chemosensitive patients with low CCL2 levels had a good overall survival ($P = 0.038$, Figure 2B). Therefore, we assumed that CCL2 was the key factor promoting chemoresistance in lung adenocarcinoma patients. To verify this further, CCL2 levels in tissues and serum from lung adenocarcinoma patients with chemosensitization and chemoresistance were measured. CCL2 mRNA expression was significantly lower in chemosensitive than in chemoresistant patients ($P < 0.01$, Figure 2C). CCL2 levels were significantly higher in serum from chemoresistant patients than in that from chemosensitive patients ($P < 0.001$, Figure 2D). We analyzed the relationship between CCL2 expression and the survival of lung adenocarcinoma patients. Patients with high CCL2 levels had a significantly worse survival rate ($P = 0.023$, Figure 2E, 2F). Together, these results indicate that CCL2 is a prognostic indicator in lung adenocarcinoma patients, and that it contributes to cisplatin-based chemotherapy resistance.

CCL2 enhances lung adenocarcinoma cell resistance to cisplatin *in vitro*

Next, we evaluated the effect of CCL2 on the chemoresistance of lung adenocarcinoma cells *in vitro*. The CCL2 stable knockdown A549/Cis cell line was successfully constructed, and was verified by qPCR analysis of CCL2 mRNA expression. CCL2 mRNA expression was significantly lower in shCCL2 A549/Cis cells than in controls ($P < 0.001$, Figure 3A). The expression of resistance-related genes was lower in shCCL2 A549/Cis cells than in controls ($P < 0.05$, Figure 3B). The proliferative ability of shCCL2 A549/Cis cells was significantly reduced compared to controls ($P < 0.05$, Figure 3C). After cisplatin treatment, shCCL2 A549/Cis cell viability was further reduced ($P < 0.01$, Figure 3C). Moreover, we found the apoptosis of shCCL2 A549/Cis cells was significantly higher than in the controls ($P < 0.05$, Figure 3D). The level of apoptosis in shCCL2 A549/Cis cells treated with cisplatin was higher than in those that were not treated with cisplatin ($P < 0.01$, Figure 3D).

Cancer stem cells are one of the key characteristics of chemoresistance in tumor cells. We therefore investigated the stemness of A549/Cis cells before and after CCL2 knockdown. Sphere-forming efficiency was significantly reduced after CCL2 knockdown in A549/Cis cells ($P < 0.001$, Figure 3E). Further, CSC-related gene expression was significantly lower in shCCL2 A549/Cis cells than in A549/Cis cells (Figure 3F). These findings demonstrate that CCL2 can enhance the chemoresistance of lung adenocarcinoma cells to cisplatin.

Chemoresistant lung adenocarcinoma cell-derived CCL2 promotes macrophage recruitment and polarization, which further mediates chemoresistance

CCL2 can promote monocyte recruitment to the tumor site, and mediate monocyte differentiation into M2 macrophages [16,17]. We therefore investigated the effect of lung adenocarcinoma cell-derived CCL2 on monocyte recruitment and macrophages polarization. THP-1 cells migrated faster in A549/Cis cell supernatants than in A549 cell supernatants ($P < 0.01$, Figure 4A). After CCL2-inhibitor treatment, the migration rates of THP-1 cells in the supernatants of both A549/Cis and A549 cells were significantly reduced ($P < 0.05$, Figure 4A). Thereafter, THP-1 cells were co-cultured with A549/Cis or A549 cells, and the proportions of $CD163^+CD14^+$ macrophages (mainly as M2 macrophages) before and after treatment with the CCL2 inhibitor were analyzed by flow cytometry. $CD163^+CD14^+$ macrophage frequency was significantly higher following co-culture with A549/Cis cells than following co-culture with A549 cells ($P < 0.05$, Figure 4B). After CCL2-inhibitor treatment, $CD163^+CD14^+$ macrophage significantly reduced relative to its frequency before CCL2-inhibitor treatment ($P < 0.05$, Figure 4B). The expression of anti-inflammatory cytokines IL-10 and TGF-b was significantly higher in macrophages co-cultured with A549/Cis cells than in those co-cultured with A549 cells ($P < 0.05$, Figure 4C). However, the expression of pro-inflammatory factors IFN-g and TNF-a in macrophages co-cultured with A549/Cis cells was lower than in macrophages co-cultured with A549 cells ($P < 0.05$, Figure 4C). The expression of IL-10 and TGF-b was reduced, and that of IFN-g and TNF-a was increased, after CCL2-inhibitor treatment ($P < 0.05$, Figure 4C). These results suggest that chemoresistant lung adenocarcinoma cell-derived CCL2 promotes recruitment of monocytes and polarization of M2 macrophages.

To further evaluate whether or not M2 macrophages affect lung adenocarcinoma chemoresistance, we investigated the effect of M2 macrophages on tumor cell proliferation, migration, and angiogenesis. A549 cells co-cultured with the supernatants of M2 macrophages polarized by A549/Cis cells had higher cell proliferative ability (Figure 4D), faster migration (Figure 4E), and higher angiogenesis (Figure 4F) than those co-cultured with the supernatants of M2 macrophages polarized by A549 cells and medium alone as a control group. Further, the expression of CCL2 and CD163 in chemoresistant lung adenocarcinoma tissues, assessed by immunohistochemistry, was significantly higher than that in tissues from chemosensitive patients (Figure 4G). Therefore, this indicates that chemoresistant lung adenocarcinoma cell-derived CCL2 promotes monocyte recruitment and polarization into M2 macrophages, which further mediates lung adenocarcinoma chemoresistance.

c-Fos is required for CCL2-enhanced chemoresistance of lung adenocarcinoma

To understand the underlying mechanism of CCL2-mediated chemoresistance, we analyzed the transcription factors in lung adenocarcinoma cells by RT^2 profiler PCR array. The c-Fos expression level in A549/Cis cells was elevated compared to that in A549 cells (Figure 5A). To verify this, c-Fos expression in A549/Cis and A549 cells was analyzed by qPCR. The mRNA expression of c-Fos was higher in A549/Cis cells than in A549 cells ($P < 0.001$, Figure 5B). To further validate the high c-Fos level in resistant lung adenocarcinoma cells, we induced A549 cells to resistant cells with cisplatin treatment. Ninety days after

treatment, c-Fos expression was significantly higher in these cisplatin-induced resistant A549 cells than in the controls ($P < 0.05$, Figure 5C).

Next, to evaluate whether CCL2-enhanced chemoresistance in lung adenocarcinoma cells is mediated by c-Fos, we further analyzed the association between CCL2 and c-Fos in lung adenocarcinoma data obtained from The Cancer Genome Atlas (TCGA) dataset. CCL2 was closely associated with c-Fos (P = 0.015, Figure 5D). A549/Cis cells were then infected with si-c-Fos to inhibit c-Fos expression (Figure 5E), to evaluate the change in CCL2 expression in A549/Cis cells. As expected, after downregulation of c-Fos expression in A549/Cis cells, CCL2 expression was significantly reduced compared to that in the controls (P < 0.001, Figure 5F). Further, A549/Cis cell proliferative ability was attenuated after treatment with si-c-Fos (P < 0.001, Figure 5G). To investigate whether c-Fos physically binds to the promoter region of CCL2, a qCHIP assay was performed using the A549/Cis and A549 cells. The CCL2 promoter region had greater c-Fos enrichment in A549/Cis cells than in the controls (P < 0.05), revealing that c-Fos is indeed located in the CCL2 promoter region in A549/Cis cells (Figure 5H-5J). These findings indicate that the involvement of c-Fos might promote chemoresistance during CCL2 expression in lung adenocarcinoma cells.

CCL2 blockade suppresses tumor progression and restores cisplatin sensitivity in lung adenocarcinoma

To evaluate the *in vivo* function of CCL2, the shCCL2, and the shRNA controls A549/Cis cells were injected subcutaneously into nude mice, and tumor growth was monitored twice per week. When tumor volumes reached 250 mm^3, cisplatin was administrated (3 mg/kg, i.p.) once per week. After two weeks of cisplatin treatment, the mice were sacrificed. Three days before the mice were sacrificed, human $CD14^+$ cells (5×10^6 cells) were transplanted into them by the caudal vein (Figure 6A). We found that tumor volume was dramatically reduced in the shCCL2 group compared to the control group ($P < 0.05$, Figure 6B). A significant reduction in tumor growth was detected in shCCL2 cell-derived xenografts following cisplatin administration, relative to the control groups, suggesting that shCCL2 A549/Cis cells enhanced chemosensitivity ($P < 0.05$, Figure 6B). However, after monocyte transfer, the tumor volume of the shCCL2 group treated with cisplatin was unchanged compared to the group without monocyte transfer (Figure 6B). Meanwhile, the final tumor volume results were measured (Figure 6C). Tumor weights were examined after the mice were sacrificed; the results were similar to those for tumor volume (Figure 6D). Last, to evaluate the effect of CCL2 depletion on monocyte recruitment to the tumor site, we investigated GFP-labeled monocyte infiltration in the xenograft tumor tissues, using flow cytometry. CCL2-knockdown significantly reduced macrophage infiltration in xenograft tissues ($P < 0.05$, Figure 6E). Accordingly, these results imply that CCL2 blockade of suppresses tumor progression and restores cisplatin sensitivity in lung adenocarcinoma.

Discussion

Non-small-cell lung cancer, of which lung adenocarcinoma is a subtype, accounts for about 80 % of lung cancer cases [18]. The currently used chemotherapeutic or targeted therapeutic drugs inevitably develop drug resistance after a period of application, presenting an obstacle to lung adenocarcinoma therapy.

Cisplatin has been used for decades as first-line chemotherapy for lung adenocarcinoma. Cisplatin's main drawback is that, following treatment, those cancer cells that evade apoptosis become resistant, leading to poor prognosis [19]. Cancer cells develop cisplatin resistance via various mechanisms, such as increasing cell growth and development, repairing DNA damage, and stimulating endocytosis, although many other factors in the immunosuppressive TME can contribute to chemoresistance. The aim of this study was to explore the molecular mechanisms whereby the TME regulates lung adenocarcinoma chemoresistance, to identify potential targets for overcoming resistance. Our findings highlight the importance of the role of CCL2 in controlling c-Fos-induced chemoresistance in lung adenocarcinoma. Accordingly, the c-Fos–CCL2 axis might provide a potential molecular target for lung adenocarcinoma therapy.

Chemokines are important in the migration of leukocytes [20, 21]. The upregulation of chemokines is closely related to tumor progression, angiogenesis, tumor invasion and metastasis [22–24], and there is much experimental evidence that chemokines contribute cancer chemoresistance. B lymphocytes, which can be recruited by CXCL13 into the tumor site, produce lymphotoxins, which promote castration-resistant prostate cancer by activating the IKKα–Bmi1 module in prostate cancer stem cells [25, 26]. Steinberg *et al*. found that myeloid-derived suppressor cells promote BRAF kinase inhibitor (BRAFi) resistance in melanoma cells, by activating the MAPK signaling pathway to induce downstream CCL2 production. MDSC depletion/blocking (via anti-Gr-1 and CCR2 antagonists) can inhibit the growth of BRAFi-resistant tumors [27]. In addition, Ly6Clo monocytes drive immunosuppression and confer resistance to anti-VEGFR2 cancer therapy in colorectal cancer (CRC). CX3CR1 is essential for the migration of Ly6Clo monocytes to mouse CRC tumors [28]. Similarly, we identified a close association between CCL2 and drug resistance: CCL2 enhanced cisplatin-resistance in lung adenocarcinoma cells. Moreover, lung adenocarcinoma cell-derived CCL2 promoted the recruitment and polarization of monocytes into M2 macrophages, which further induced resistance.

Binding of CCL2 to CCR2 promotes the recruitment of monocytes to primary tumors and metastases [29]. In primary sclerosing cholangitis, senescent and BV6-treated human cholangiocytes released monocyte chemoattractant CCL2, which promoted monocyte recruitment to the tissue site [30]. Interestingly, high levels of CCL2 were detected within the follicular lymphoma-cell niche, and CCL2 is overexpressed by follicular lymphoma-mesenchymal stromal cells; this is consistent with the capacity of these cells to recruit monocytes more efficiently than healthy donor-mesenchymal stromal cells [31]. Moreover, in liver disease, the chemokine pathways that involve CCR2 or CCL2 modulate monocyte recruitment or macrophage polarization and differentiation [16]. CCL2 stimulates macrophage proliferation and polarization in multiple myelomas [17, 32]. Our findings are consistent with this: we found that CCL2 promoted monocyte recruitment into tumor sites, and polarization of monocytes into M2 macrophages.

Our results showed that c-Fos might be required in order for CCL2 expression to enhance chemoresistance of lung adenocarcinoma. The association between c-Fos and drug resistance has previously been reported. Overexpression of *c-Fos* in human ovarian cancer cell lines can lead to cisplatin resistance. In addition, the expression of the c-Fos gene may affect cisplatin sensitivity, and c-Fos

antisense oligonucleotide alone, or in combination with cisplatin, can effectively kill parental and cisplatin-resistant ovarian cancer cells [33]. c-Fos increased the expression of P-gp and mdr1 in HEp-2/chemotherapeutic vincristine cells, and enhanced the efflux function of these cells, thereby contributing to the development of multidrug resistance [34]. c-Fos in platinum-resistant cells was up-regulated early in the transcriptional process after 5-FdU–ECyd treatment [35]. For a wide range of leukemias, Kesarwani *et al*. [36] reported that growth-factor-induced c-Fos expression conferred intrinsic resistance to tyrosine-kinase-inhibitor treatment, because the c-Fos expression levels determined the threshold for tyrosine kinase inhibitor efficacy.

Targeting the c-Fos–CCL2 axis in tumors may provide a novel potential therapeutic strategy for controlling lung adenocarcinoma. Li *et al*. [37] found that CCL2 was overexpressed in human liver cancers and was prognostic for patients with hepatocellular carcinoma. Blockade of CCL2/CCR2 signalling via CCR2 knockout, or using a CCR2 antagonist, inhibited malignant growth and metastasis, reduced postsurgical recurrence, and enhanced survival, suggesting the translational potential of CCL2/CCR2 blockade for treating hepatocellular carcinoma [37]. Moreover, anti-CCL2 antibody is effective in treating mouse hepatocellular carcinoma by blocking the CCL2–CCR2 axis [38]. In a mouse model, DNA vaccines targeting Fos-associated antigen 1 can induce $CD8^+$ T cell-mediated specific immunity, eradicating spontaneous and experimental lung cancer metastasis; these vaccines are equally effective in breast cancer metastasis models [39]. In the current study, we investigated tumor growth *in vitro* using si-c-Fos cells and *in vivo* using shCCL2 cells, and we found that the involvement of c-Fos in CCL2 expression in lung adenocarcinoma cells might promote chemoresistance. Further, we found that CCL2 blockade suppressed tumor progression and restored cisplatin sensitivity in lung adenocarcinoma, suggesting that the c-Fos–CCL2 axis may be a potential therapeutic target for lung adenocarcinoma.

Conclusions

In summary, high levels of CCL2 mediated chemoresistance in lung adenocarcinoma via the action of c-Fos. CCL2 blockade suppressed tumor progression and restored cisplatin sensitivity in lung adenocarcinoma. Therefore, therapeutic strategies that target c-Fos/CCL2 axis could represent an effective approach in lung adenocarcinoma treatment.

Declarations

Ethics approval and consent to participate

The research protocol was reviewed and approved by the Ethics Committee of The First Affiliated Hospital of Zhengzhou University, and written informed consent was obtained from each patient included in the study. All procedures involving animals were performed according to the guidelines of the Association for the Assessment and Accreditation of Laboratory Animal Care International.

Consent for publication

No conflict of interest exits in the submission of this manuscript, and manuscript is approved by all authors for publication.

Availability of data and materials

The datasets supporting the findings of this study are included within the article.

Competing interests: The authors confirm that there are no conflicts of interest.

Funding

This study was supported by grants from the National Natural Science Foundation of China (No.81771781, No.81602024, No.81872410), Funding from State's Key Project of Research and Development Plan (No. 2016YFC1303501), International Research Cooperation Grant from Science and Technology Department of Henan Province (No.162102410059), Research Grant from the Ministry of Public Health (No.201501004).

Author contributions:

DW, LY and YL participated in the research design and coordination and helped to draft the manuscript. DW and YL conducted the experiments. LC and ZS carried out the immunoassays. LW and ZS contributed the clinical sample collection. KZ, JH, and JL performed the data analysis. All authors read and approved the final manuscript.

Acknowledgments

Not applicable.

Data availability:

The datasets supporting the findings of this study are included within the article.

References

1. Holohan C, Van Schaeybroeck S, Longley DB, Johnston PG. Cancer drug resistance: an evolving paradigm. Nat Rev Cancer 2013; 13: 714-726.
2. McMillin DW, Negri JM, Mitsiades CS. The role of tumour-stromal interactions in modifying drug response: challenges and opportunities. Nat Rev Drug Discov 2013; 12: 217-228.
3. Velaei K, Samadi N, Barazvan B, Soleimani Rad J. Tumor microenvironment-mediated chemoresistance in breast cancer. Breast (Edinburgh, Scotland) 2016; 30: 92-100.
4. Villanueva MT. Cell signalling: Stuck in the middle of chemoresistance and metastasis. Nature reviews Clinical oncology 2012; 9: 490.

5. Liu XD, Hoang A, Zhou L, et al. Resistance to Antiangiogenic Therapy Is Associated with an Immunosuppressive Tumor Microenvironment in Metastatic Renal Cell Carcinoma. Cancer Immunol Res. 2015, 3(9):1017-29.
6. Perrotta C, Cervia D, Di Renzo I, et al. Nitric Oxide Generated by Tumor-Associated Macrophages Is Responsible for Cancer Resistance to Cisplatin and Correlated With Syntaxin 4 and Acid Sphingomyelinase Inhibition. Front Immunol. 2018, 29;9:1186.
7. Hartmann TN, Burger JA, Glodek A, Fujii N, Burger M. CXCR4 chemokine receptor and integrin signaling co-operate in mediating adhesion and chemoresistance in small cell lung cancer (SCLC) cells. Oncogene 2005; 24: 4462-4471.
8. Calinescu AA, Yadav VN, Carballo E, Kadiyala P, Tran D, Zamler DB et al. Survival and Proliferation of Neural Progenitor-Derived Glioblastomas Under Hypoxic Stress is Controlled by a CXCL12/CXCR4 Autocrine-Positive Feedback Mechanism. Clinical cancer research : an official journal of the American Association for Cancer Research 2017; 23: 1250-1262.
9. Gil M, Seshadri M, Komorowski MP, Abrams SI, Kozbor D. Targeting CXCL12/CXCR4 signaling with oncolytic virotherapy disrupts tumor vasculature and inhibits breast cancer metastases. Proceedings of the National Academy of Sciences of the United States of America 2013; 110: E1291-1300.
10. Park YH, Sohn SK, Kim JG, Lee MH, Song HS, Kim MK et al. Interaction between BCL2 and interleukin-10 gene polymorphisms alter outcomes of diffuse large B-cell lymphoma following rituximab plus CHOP chemotherapy. Clinical cancer research : an official journal of the American Association for Cancer Research 2009; 15: 2107-2115.
11. Heinecke JL, Ridnour LA, Cheng RY, Switzer CH, Lizardo MM, Khanna C et al. Tumor microenvironment-based feed-forward regulation of NOS2 in breast cancer progression. Proceedings of the National Academy of Sciences of the United States of America 2014; 111: 6323-6328.
12. Bid HK, Kibler A, Phelps DA, Manap S, Xiao L, Lin J et al. Development, characterization, and reversal of acquired resistance to the MEK1 inhibitor selumetinib (AZD6244) in an in vivo model of childhood astrocytoma. Clinical cancer research : an official journal of the American Association for Cancer Research 2013; 19: 6716-6729.
13. Korkaya H, Liu S, Wicha MS. Regulation of cancer stem cells by cytokine networks: attacking cancer's inflammatory roots. Clinical cancer research: an official journal of the American Association for Cancer Research 2011; 17: 6125-6129.
14. Li L, Yang L, Wang L, Wang F, Zhang Z, Li J, Yue D, Chen X, Ping Y, Huang L, Zhang B, Zhang Y. Impaired T cell function in malignant pleural effusion is caused by TGF-β derived predominantly from macrophages. Int J Cancer, 2016, 139(10):2261-2269.
15. Ichiyama K1, Sekiya T, Inoue N, et al. Transcription factor Smad-independent T helper 17 cell induction by transforming-growth factor-β is mediated by suppression of eomesodermin. Immunity. 2011;34(5):741-54.
16. Tacke F. Targeting hepatic macrophages to treat liver diseases. J Hepatol, 2017, 66(6):1300-1312.

17. Yang L, Zhang Y. Tumor-associated macrophages: from basic research to clinical application. J Hematol Oncol, 2017, 10(1):58.
18. Haghgoo SM, Allameh A, Mortaz E, Garssen J, Folkerts G, Barnes PJ, et al. Pharmacogenomics and targeted therapy of cancer: focusing on non-small cell lung cancer. Eur J Pharmacol, 2015, 754:82-91.
19. Waissbluth S, Daniel SJ. Cisplatin-induced ototoxicity: transporters playing a role in cisplatin toxicity. Hear Res, 2013, 299:37-45.
20. Baggiolini M. Chemokines and leukocyte traffic. Nature, 1998, 392:565-568.
21. Duda DG, Kozin SV, Kirkpatrick ND, Xu L, Fukumura D, Jain RK. CXCL12 (SDF1alpha)-CXCR4/CXCR7 pathway inhibition: an emerging sensitizer for anticancer therapies? Clinical cancer research : an official journal of the American Association for Cancer Research, 2011, 17:2074-2080.
22. Seifert L, Werba G, Tiwari S, Giao Ly NN, Alothman S, Alqunaibit D, et al. The necrosome promotes pancreatic oncogenesis via CXCL1 and Mincle-induced immune suppression. Nature, 2016, 532(7598):245-249.
23. Yang J, Kumar A, Vilgelm AE, Chen SC, Ayers GD, Novitskiy SV, Joyce S, Richmond A. Loss of CXCR4 in Myeloid Cells Enhances Antitumor Immunity and Reduces Melanoma Growth through NK Cell and FASL Mechanisms. Cancer Immunol Res, 2018, pii: canimm.0045.2018.
24. Liu LZ, Zhang Z, Zheng BH, Shi Y, Duan M, Ma LJ, et al. CCL15 recruits suppressive monocytes to facilitate immune escape and disease progression in hepatocellular carcinoma. Hepatology, 2018 Aug 2. doi: 10.1002/hep.30134. [Epub ahead of print]
25. Ammirante M, Luo JL, Grivennikov S, Nedospasov S, Karin M. B-cell-derived lymphotoxin promotes castration-resistant prostate cancer. Nature, 2010, 464:302-305.
26. Ammirante M, et al. An IKKalpha-E2F1-BMI1 cascade activated by infiltrating B cells controls prostate regeneration and tumor recurrence. Genes Dev, 2013, 27:1435-1440.
27. Steinberg SM, Shabaneh TB, Zhang P, Martyanov V, Li Z, Malik BT, et al. Myeloid Cells That Impair Immunotherapy Are Restored in Melanomas with Acquired Resistance to BRAF Inhibitors. Cancer Res, 2017, 77(7):1599-1610.
28. Jung K, Heishi T, Khan OF, Kowalski PS, Incio J, Rahbari NN, et al. Ly6Clo monocytes drive immunosuppression and confer resistance to anti-VEGFR2 cancer therapy. J Clin Invest, 2017, 127(8):3039-3051.
29. Franklin RA, Liao W, Sarkar A, Kim MV, Bivona MR, Liu K, Pamer EG, Li MO. The cellular and molecular origin of tumor-associated macrophages. Science, 2014, 344:921-925.
30. Guicciardi ME, Trussoni CE, Krishnan A, Bronk SF, Lorenzo Pisarello MJ, O'Hara SP, et al. Macrophages contribute to the pathogenesis of sclerosing cholangitis in mice. J Hepatol, 2018, 69(3):676-686.
31. Guilloton F, Caron G, Ménard C, Pangault C, Amé-Thomas P, Dulong J, De Vos J, Rossille D, Henry C, Lamy T, Fouquet O, Fest T, Tarte K. Mesenchymal stromal cells orchestrate follicular lymphoma cell

niche through the CCL2-dependent recruitment and polarization of monocytes. Blood, 2012, 119(11):2556-2567.

32. Li Y, Zheng Y, Li T, Wang Q, Qian J, Lu Y, Zhang M, Bi E, Yang M, Reu F, et al. Chemokines CCL2, 3, 14 stimulate macrophage bone marrow homing, proliferation, and polarization in multiple myeloma. Oncotarget, 2015, 6:24218-24229.
33. Moorehead RA, Singh G. Influence of the proto-oncogene c-Fos on cisplatin sensitivity. Biochem Pharmacol, 2000, 59(4):337-345.
34. Li G, Hu X, Sun L, Li X, Li J, Li T, Zhang X. C-Fos upregulates P-glycoprotein, contributing to the development of multidrug resistance in HEp-2 laryngeal cancer cells with VCR-induced resistance. Cell Mol Biol Lett, 2018, 23:6.
35. Schott S, Wimberger P, Klink B, Grützmann K, Puppe J, Wauer US, Klotz DM, Schröck E, Kuhlmann JD. The conjugated antimetabolite 5-FdU-ECyd and its cellular and molecular effects on platinum-sensitive vs. -resistant ovarian cancer cells in vitro. Oncotarget, 2017, 8(44):76935-76948.
36. Kesarwani M, Kincaid Z, Gomaa A, Huber E, Rohrabaugh S, Siddiqui Z, Bouso MF, Latif T, Xu M, Komurov K, Mulloy JC, Cancelas JA, Grimes HL, Azam M. Targeting c-Fos and DUSP1 abrogates intrinsic resistance to tyrosine-kinase inhibitor therapy in BCR-ABL-induced leukemia. Nat Med, 2017, 23(4):472-482.
37. Li X, Yao W, Yuan Y, Chen P, Li B, Li J, Chu R, Song H, Xie D, Jiang X, Wang H. Targeting of tumour-infiltrating macrophages via CCL2/CCR2 signalling as a therapeutic strategy against hepatocellular carcinoma. Gut, 2017, 66(1):157-167.
38. Teng KY, Han J, Zhang X, Hsu SH, He S, Wani NA, Barajas JM, Snyder LA, Frankel WL, Caligiuri MA, Jacob ST, Yu J, Ghoshal K. Blocking the CCL2-CCR2 Axis Using CCL2-Neutralizing Antibody Is an Effective Therapy for Hepatocellular Cancer in a Mouse Model. Mol Cancer Ther, 2017, 16(2):312-322.
39. Luo Y, Zhou H, Mizutani M, Mizutani N, Liu C, Xiang R, Reisfeld RA. A DNA vaccine targeting Fos-related antigen 1 enhanced by IL-18 induces long-lived T-cell memory against tumor recurrence. Cancer Res, 2005, 65(8):3419-3427.

Tables

Table 1. Correlation analysis between CCL2 expression level and clinical parameters of patients with lung adenocarcinoma

Patient characteristics		Number	Mean±SD	*P* value
Gender				
	Male	60	2.014±3.267	0.317
	Female	21	1.063±0.762	
Age				
	>60	42	1.931±2.779	
	<=60	39	1.615±2.962	0.114
Clinical lymph node metastasis				
	No	43	1.308±1.699	0.2785
	Yes	38	2.286±3.73	
Differentiation				
	Middle/low	51	1.861±2.659	0.045*
	High	30	1.608±3.219	
Clinical stage				
	I- II	55	1.147±0.207	0.025*
	III-IV	26	3.079 ±0.842	
Histological type				
	Adenocarcinoma	45	1.729±3.171	0.122
	Squamous carcinoma	36	1.797±2.626	

* $P < 0.05$.

Figures

Figure 1

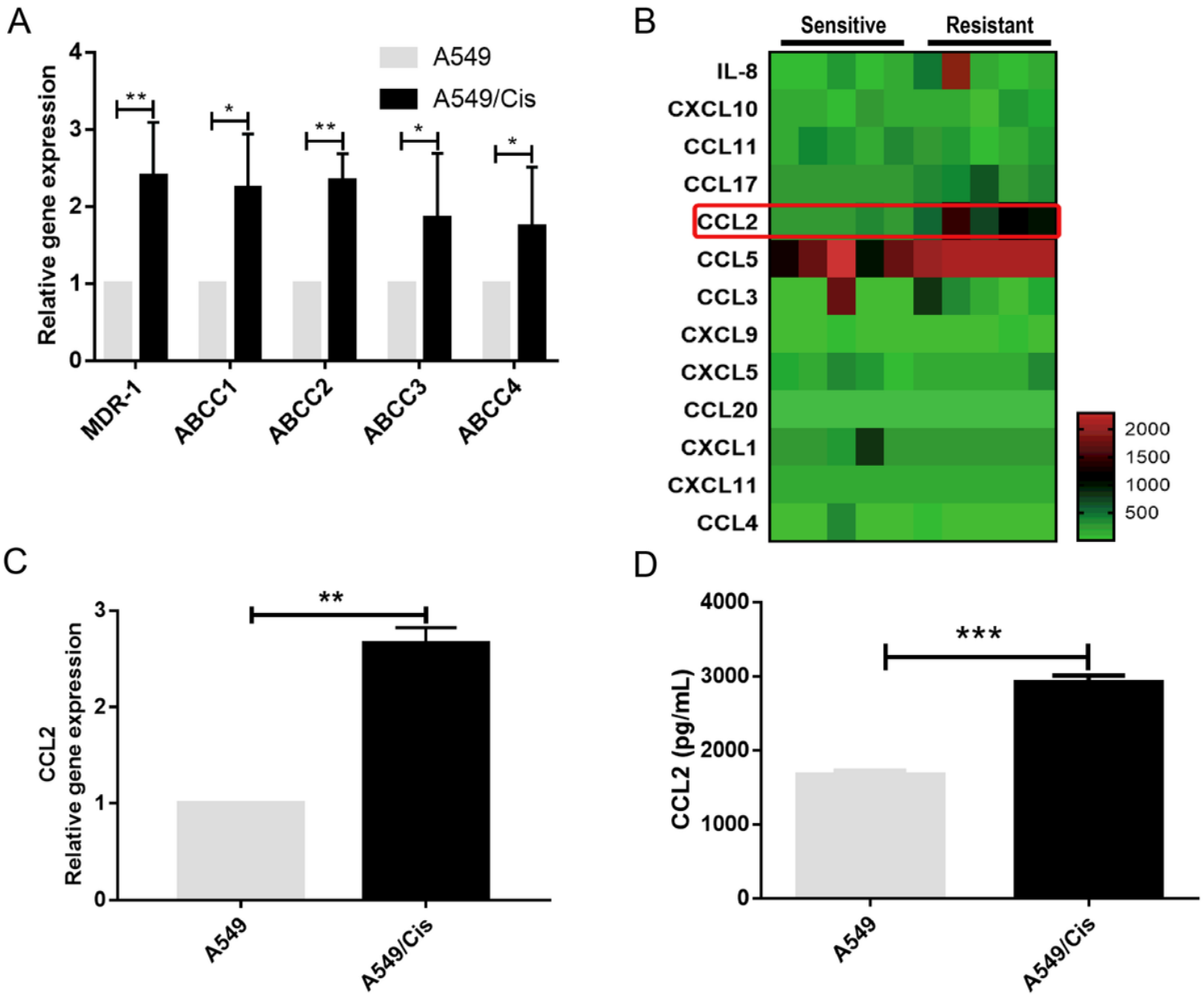

Figure 1

The level of CCL2 is elevated in lung adenocarcinoma cells with chemoresistance. A. Resistance-related gene expression levels in A549 and A549/Cis cells were analyzed by qPCR. B. Heatmap showing the concentration of 13 chemokines (pg/mL) in supernatants obtained from A549 and A549/Cis cells measured by multiplex assay. C. CCL2 relative expression in A549 and A549/Cis cells was analyzed by qPCR. D. CCL2 concentration (pg/mL) in supernatants obtained from A549 and A549/Cis cells was measured by ELISA. Results are expressed as means ± SD. * = P < 0.05; ** = P < 0.01; *** = P < 0.001.

Figure 2

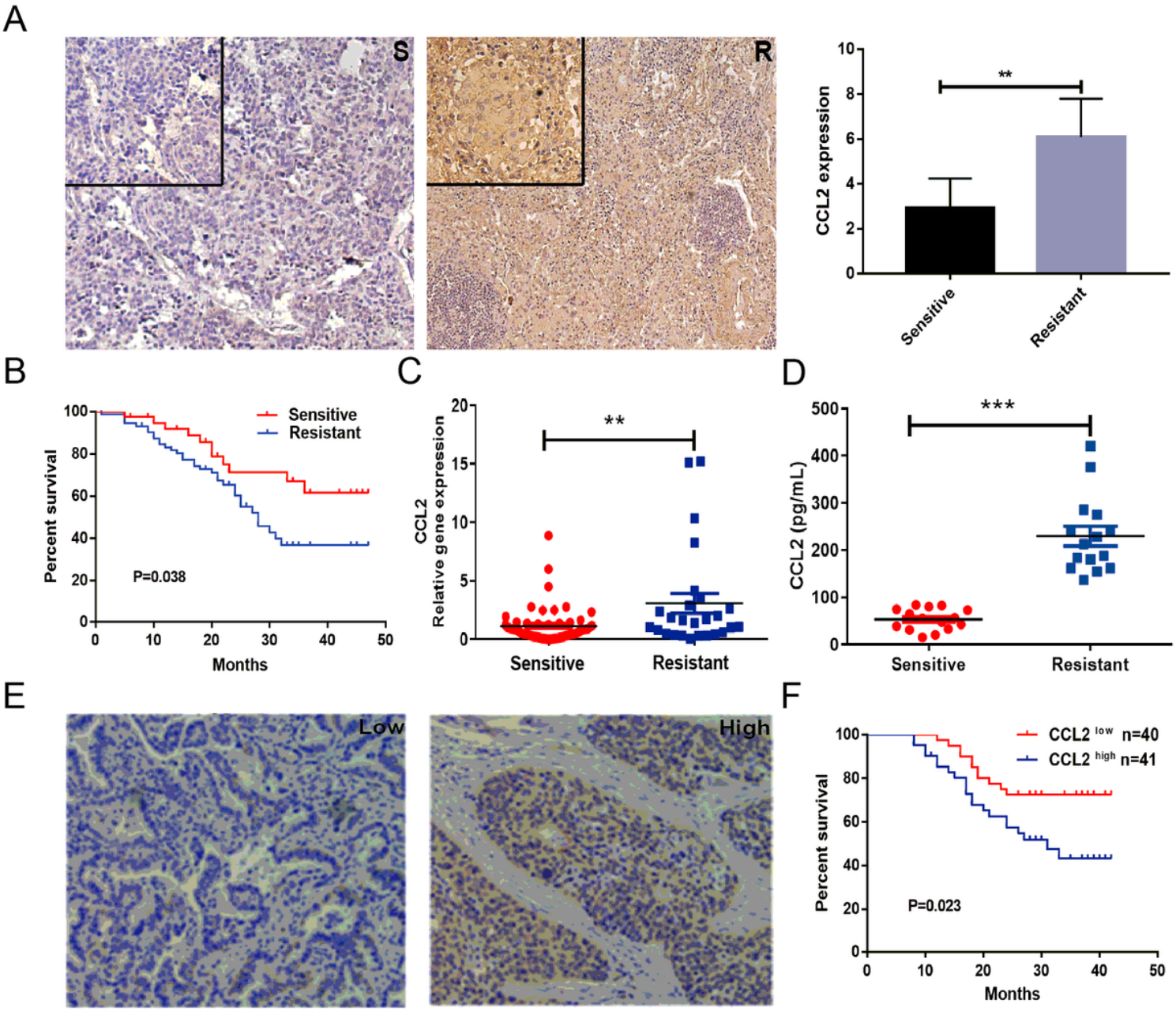

Figure 2

High CCL2 levels are closely associated with chemoresistance and poor survival in lung adenocarcinoma patients. A. CCL2 in chemosensitive and chemoresistant lung adenocarcinoma tissues was detected by immunohistochemistry (200 ×). B. Kaplan-Meier survival curves for 81 lung adenocarcinoma patients with chemosensitization or chemoresistance. C. CCL2 relative expression in chemosensitive and chemoresistant lung adenocarcinoma tissues was analyzed by qPCR. D. CCL2 concentration (pg/mL) in supernatants obtained from the tissues of chemosensitive and chemoresistant lung adenocarcinoma patients was measured by ELISA. E. CCL2 expression in lung adenocarcinoma tissues was analyzed by immunohistochemistry (200 ×). A representative analysis from one experiment is shown. F. Kaplan-Meier survival curves for 81 lung adenocarcinoma patients with lower or higher CCL2 expression

(immunohistochemical analysis). Results are expressed as means ± SD. * = P < 0.05; ** = P < 0.01; *** = P < 0.001.

Figure 3

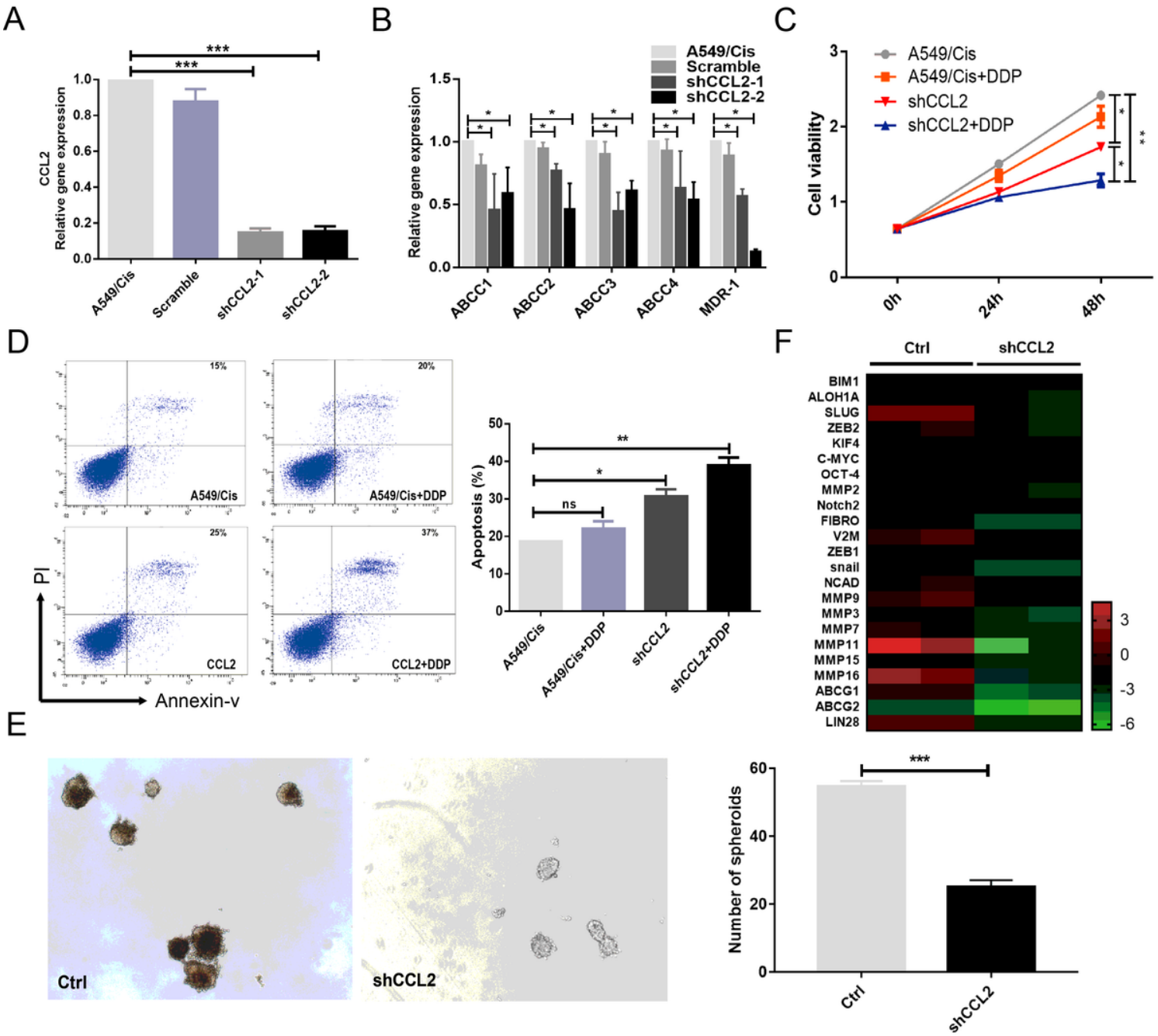

Figure 3

CCL2 enhances the resistance of lung adenocarcinoma cells to cisplatin in vitro. A. CCL2 relative expression in shCCL2 and scramble shRNA A549/Cis cells was analyzed by qPCR. B. The relative expression of resistance-related genes in shCCL2 and scramble shRNA A549/Cis cells was analyzed by qPCR. C. The viability of shCCL2 and scramble shRNA A549/Cis cells before and after cisplatin (DDP)

treatment was analyzed by CCK8 assay. D. Cell apoptosis of shCCL2 and scramble shRNA A549/Cis cells before and after treatment with cisplatin was evaluated by flow cytometry. A representative analysis from one experiment is shown. E. shCCL2 and scramble shRNA A549/Cis cells were cultured for sphere-formation assay. One representative micrograph is shown (200 ×). F. Heatmap showing the expression of stemness-related genes in shCCL2 and scramble shRNA A549/Cis cells. Results are expressed as means ± SD. * = P < 0.05; ** = P < 0.01; *** = P < 0.001; ns = non-significant.

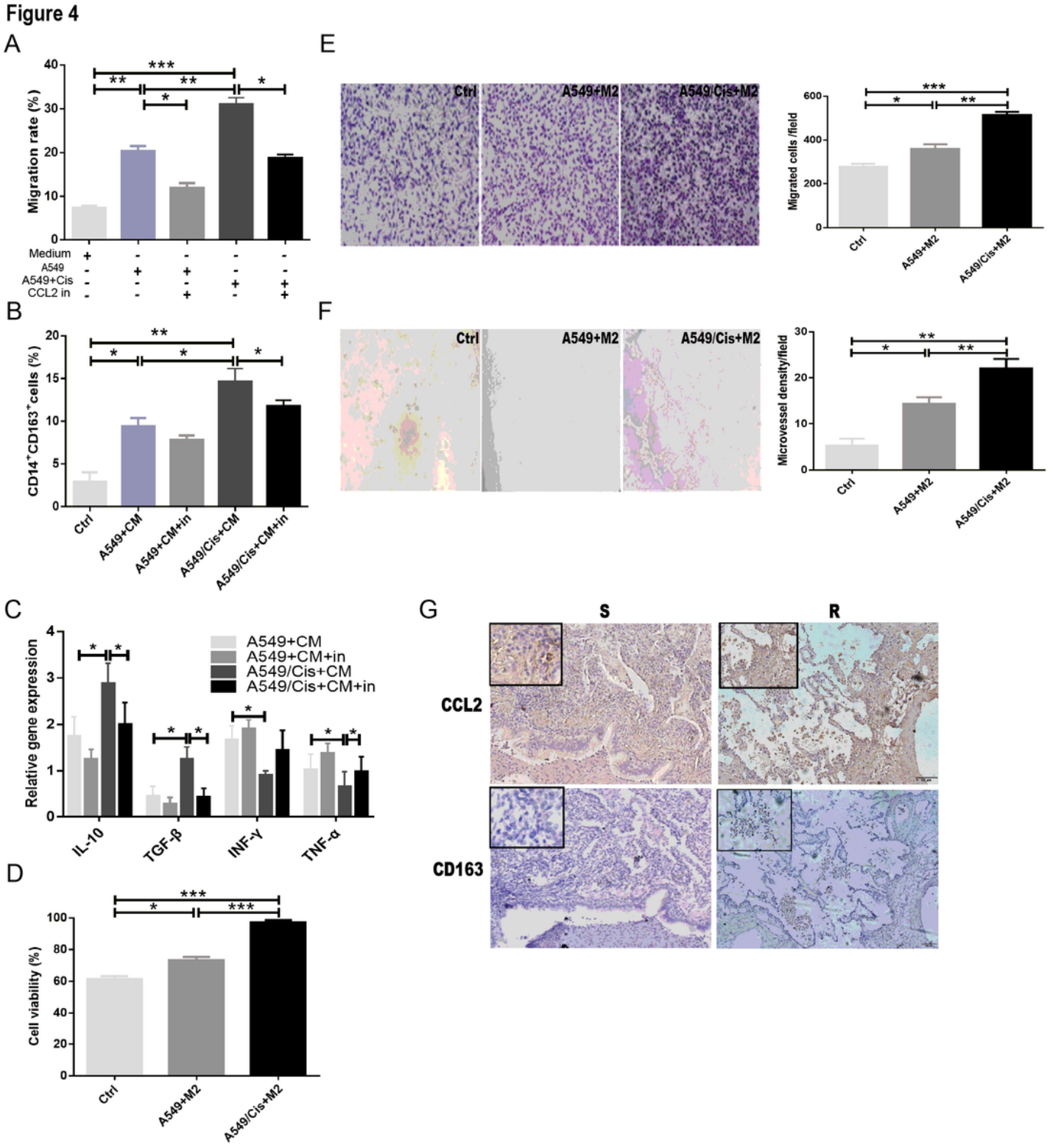

Figure 4

CCL2 derived from A549/Cis cells promotes macrophage recruitment and polarization, which further mediates chemoresistance. A. Cell migration of THP-1 cells co-cultured with the supernatants of A549 or A549/Cis cells before and after CCL2-inhibitor treatment was analyzed by transwell assay. B. The percentage of CD163+CD14+ cells in THP-1 cells co-cultured with the supernatants of A549 or A549/Cis cells before and after CCL2-inhibitor treatment was analyzed by flow cytometry. C. The relative expression of IL-10, TGF-β, IFN-γ, and TNF-αin THP-1 cells co-cultured with the supernatants of A549 or A549/Cis cells before and after CCL2-inhibitor treatment was analyzed by qPCR. D. The viability of A549 cells co-cultured with the supernatants of M2 macrophages induced by A549 or A549/Cis cells was analyzed by CCK8 assay. E. Cell migration of A549 cells co-cultured with the supernatants of M2 macrophages induced by A549 or A549/Cis cells was analyzed by transwell assay (200 ×). The results are presented as a histogram. F. HUVEC cells co-cultured with the supernatants of M2 macrophages induced by A549 or A549/Cis cells were analyzed by tube-formation assay (200 ×). The results are presented as a histogram. G. The effects of CCL2 and CD163 expression in tumor tissues from chemosensitive and chemoresistant lung adenocarcinoma patients were analyzed by immunohistochemistry (200 ×). Results are expressed as means ± SD. * = $P < 0.05$; ** = $P < 0.01$; *** = $P < 0.001$.

Figure 5

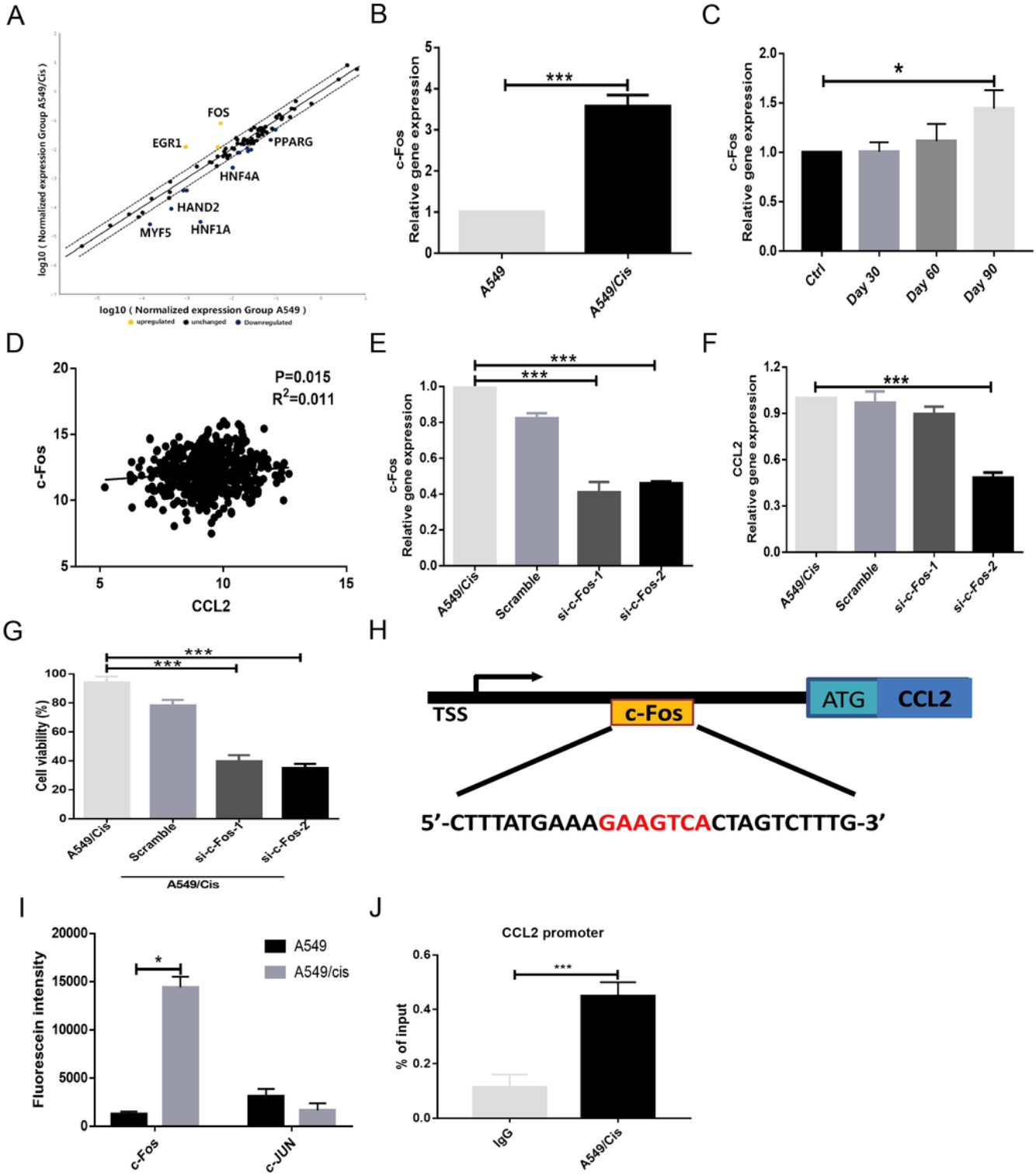

Figure 5

c-Fos regulates CCL2-enhanced chemoresistance in lung adenocarcinoma. A. The expression of transcription factors in A549 and A549/Cis cells was analyzed by RT2 Profiler PCR Array. B. The relative expression of c-Fos in A549 and A549/Cis cells was analyzed by qPCR. C. The relative expression of c-Fos in A549 cells before cisplatin treatment, and 30, 60, and 90 days after cisplatin treatment. D. Association between CCL2 and c-Fos in lung adenocarcinoma tissues, assessed using the TCGA

database. E. The relative expression of c-Fos in si-c-Fos A549/Cis cells was analyzed by qPCR. F. The relative expression of CCL2 in si-c-Fos A549/Cis cells was analyzed by qPCR. G. The viability of si-c-Fos A549/Cis cells was analyzed by CCK8 assay. H. Schematic representation of the CCL2 promoter region. “c-Fos” indicates the location of the c-Fos primer on the CCL2 promoter. I. Fluorescein intensity of c-Fos and c-JUN was measured in A549/Cis and A549 cells. J. qChIP assay was performed to evaluate c-Fos enrichment in the CCL2 promoter region of A549/Cis cells. Normal goat anti-rabbit IgG served as a negative control. Results are expressed as means ± SD. * = P < 0.05; *** = P < 0.001.

Figure 6

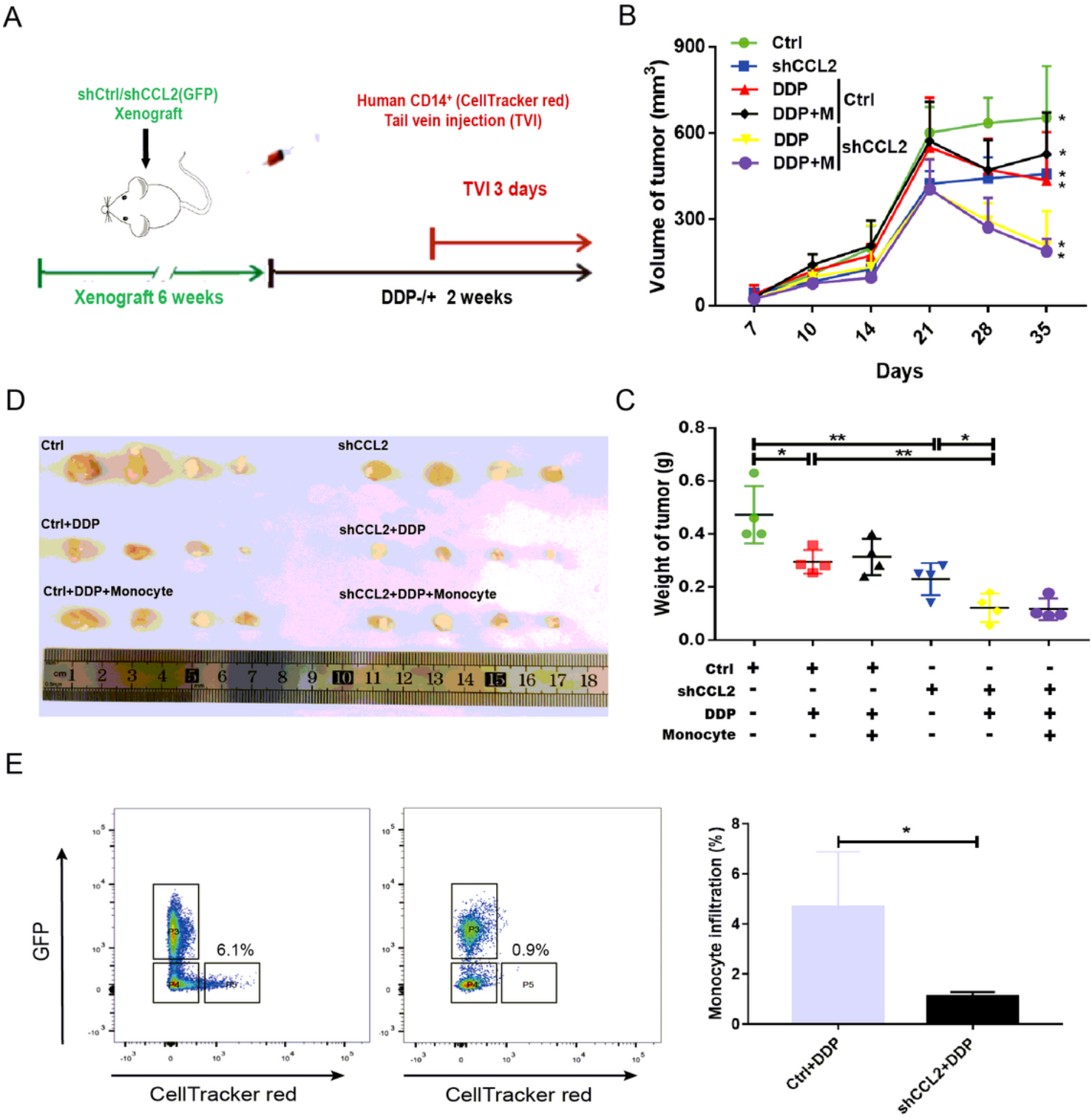

Figure 6

CCL2 blockade suppresses tumor progression and restores cisplatin sensitivity in lung adenocarcinoma in vivo. A. Illustration of the process of cell injection, cisplatin (DDP) treatment, and CD14+ cell transfer in vivo. shCCL2 or shRNA control A549/Cis cells were injected subcutaneously into nude mice, and tumor growth was monitored twice per week. When tumor volumes reached 250 mm3, cisplatin was administrated (3 mg/kg, i.p.) once per week. After two weeks of cisplatin treatment, mice were sacrificed. Three days before the mice sacrificed, human CD14+ cells (5 × 106 cells) were transplanted into them by the caudal vein. B. Tumor volumes were measured from day 7 to day 35 after cell implantation. C. Tumor volumes were measured at day 35 after cell implantation. D. Tumor weights were analyzed at day 30 after cell implantation. E. The proportion of monocytes labeled by CellTracker Red in the mouse xenograft tissue was analyzed by flow cytometry. A representative analysis from one experiment is shown. The results are presented as a histogram. Results are expressed as means ± SD. * = $P < 0.05$; ** = $P < 0.01$; ns = non-significant.